

High-resolution synchrotron radiation-based phase tomography of the healthy and epileptic brain

Christos Bikis^{*a}, Philipp Janz^b, Georg Schulz^a, Gabriel Schweighauser^c, Jürgen Hench^c, Peter Thalmann^a, Hans Deyhle^a, Natalia Chicherova^{a,d}, Alexander Rack^e, Anna Khimchenko^a, Simone E. Hieber^a, Luigi Mariani^f, Carola A. Haas^b, and Bert Müller^a

^aBiomaterials Science Center, Department of Biomedical Engineering, University of Basel, Gewerbestrasse 14, 4123 Allschwil, Switzerland; ^bExperimental Epilepsy Research, Department of Neurosurgery, University Medical Center Freiburg, Freiburg, Breisacher Strasse 64, D-79106 Freiburg i. Brsg., Germany; ^cInstitute of Pathology, Department of Neuropathology, University Hospital Basel, Schönbeinstrasse 40, 4001 Basel, Switzerland; ^dMedical Image Analysis Center, University of Basel, Gewerbestrasse 14, 4123 Allschwil, Switzerland; ^eEuropean Synchrotron Radiation Facility, Structure of Materials Group-ID19, CS 40220, F-38043, Grenoble Cedex 9, France; ^fDepartment of Neurosurgery, University Hospital Basel, Spitalstrasse 21, 4031, Basel, Switzerland

ABSTRACT

Phase-contrast micro-tomography using synchrotron radiation has yielded superior soft tissue visualization down to the sub-cellular level. The isotropic spatial resolution down to about one micron is comparable to the one of histology. The methods, however, provide different physical quantities and are thus complementary, also allowing for the extension of histology into the third dimension. To prepare for cross-sectional animal studies on epilepsy, we have standardized the specimen's preparation and scanning procedure for mouse brains, so that subsequent histology remains entirely unaffected and scanning of all samples ($n = 28$) is possible in a realistic time frame. For that, we have scanned five healthy and epileptic mouse brains at the ID19 beamline, ESRF, Grenoble, France, using grating- and propagation-based phase contrast micro-tomography. The resulting datasets clearly show the cortex, ventricular system, thalamus, hypothalamus, and hippocampus. Our focus is on the latter, having planned kainate-induced epilepsy experiments. The cell density and organization in the dentate gyrus and Ammon's horn region were clearly visualized in control animals. This proof of principle was required to initiate experiment. The resulting three-dimensional data have been correlated to histology. The goal is a brain-wide quantification of cell death or structural reorganization associated with epilepsy as opposed to histology alone that represents small volumes of the total brain only. Thus, the proposed technique bears the potential to correlate the gold standard in analysis with independently obtained data sets. Such an achievement also fuels interest for other groups in neuroscience research to closely collaborate with experts in phase micro-tomography.

Keywords: Phase-contrast micro-tomography, X-ray grating interferometry, single-distance phase retrieval, synchrotron radiation, animal studies, mouse brain, epilepsy

1. INTRODUCTION

1.1 State-of-the art and open challenges in brain imaging

In terms of imaging and morphological analysis, the nervous system presents medical practitioners and researchers with considerable challenges. The brain, being completely enclosed inside the skull, is more difficult to image and access than most organs, especially if we consider the *in vivo* situation. In addition, the physical properties of the nervous tissue are such that the non-destructive, three-dimensional imaging technique with the true micrometer resolution, i.e. X-ray computed tomography in the well-established absorption contrast mode, is inappropriate for thorough examination. Among the visualization tools for the nervous system, histology is the *ex vivo* gold standard in terms of lateral spatial resolution and functional information provided by specialized stains including immunochemistry.

*christos.bikis@unibas.ch; phone +41 61 207 54 34; www.bmc.unibas.ch

The need for a three-dimensional visualization of the mouse brain though is evident, given the importance of brain lamination, also regulating the properties of neuronal synapses, the basis of the brain circuitry. Visualization by serial histological sectioning and subsequent reconstruction is a time-consuming procedure and error-prone. It also presents a number of technical challenges in assembling a three-dimensional image, given the relatively common tissue loss in between sections. Consequently, recent optical clearance methods preceding fluorescence microscopy, like the CLARITY protocol [1], are gaining popularity despite their shortcomings. Optical clearing of tissue is technically demanding, taking up to several days and restricted to *ex vivo* characterization. Moreover, the expression of fluorescent marker proteins is most usually necessary but not always feasible. The alternative of antibody staining needs days of incubation and is excluded for specimens thicker than a couple of millimeters due to low permeability. Limitations also exist in the number of antibodies that can be applied to a single specimen. Cleared tissue cannot be stored for long periods of time, because the intensity of fluorescent proteins is reduced over time. Lastly, after optical clearing, histological processing of the tissue is no longer possible [2].

1.2 Synchrotron-radiation micro-tomography as histology complement

With these medically driven challenges in mind, the method of micro computed tomography and most prominently synchrotron radiation phase tomography is the prime candidate for complementing the gold standard of *ex vivo* imaging, i.e. histology. Phase tomography is a recently better and better established imaging method that yields far superior contrast for soft biological tissues than conventional X-ray tomography in absorption contrast mode [3, 4]. Being a non-destructive method it can be performed before any histological processing, not affecting the subsequent workup, while offering isotropic resolution at the micrometer scale and even below [5]. The aim of this pilot study is to prove the merit of histology-validated phase tomography for selected nervous system components down to individual cells, when used for complementing existing visualization procedures in biomedical applications. The three-dimensional visualization of ensembles of cells with isotropic micrometer resolution especially correlated with the established histology will be useful both for neuroscience research and in the clinical setting.

1.3 The mouse as a model organism

For the course of this project, we intend to use phase tomography to visualize the three-dimensional arrangement of individual cells in the entire mouse brain hemisphere. The mouse is one of the most prevalent model animals for research and medical studies. The high homology with humans, the complete sequencing of its reference genome and high reproduction rates make the laboratory mouse the prime choice for genetically engineered model animals. Combined with their small size and relative ease of reproducing, an unprecedented number of mouse models have been developed. Amongst them are suitable setups for neuroscience studies on the mechanisms of memory and learning, anxiety and fear, depression, epilepsy, and schizophrenia [6-9]. The histology-correlated visualization will offer a three-dimensional map of the mouse brain with cellular resolution, benchmarked on a well-characterized mouse model of medial temporal lobe epilepsy (MTLE).

1.4 Medial temporal epilepsy (MTLE) and hippocampal sclerosis

Choosing the medial temporal epilepsy (MTLE) mouse model for benchmarking our planned mouse brain visualization is mainly based on medical criteria, including clinical severity and ample opportunities for research both in the areas of disease etiology and therapeutics. These could substantially benefit by the true micrometer resolution in the three orthogonal directions. MTLE is the most common form of focal intractable epilepsies and resistance to pharmacological therapy is common, with amygdalo-hippocampectomy being then the therapeutic option of choice [10]. MTLE has from early on been correlated with hippocampal sclerosis, the morphological abnormality of pyramidal neuron loss and subsequent glial scarring in the *Cornu ammonis* (CA) region. Histological anomalies also include granule cell dispersion (GCD) of the *dentate gyrus* (DG), loss of large hilar neurons and mossy fiber sprouting [11-13]. Proper layering, depending on three-dimensional arrangement of hippocampal cells has been found to both affect survival and be instrumental in regulating neuronal circuitry, leading to recess or consolidation of epilepsy [14-16]. Thus, a three-dimensional visualization down to the level of individual neurons can substantially aid in promoting relevant research. Recent scans of human brain tissue at synchrotron radiation facilities have depicted whole cells in human cerebellum and hippocampal samples, identifying details of the Purkinje neurons [3, 17]. Considering the special structure of the hippocampus, with the dentate gyrus and Ammon's Horn showing up in phase tomography, the model of kainite (KA)-induced MTLE is technically suitable [18]. A scan of the whole brain hemisphere will facilitate the accurate spatial orientation based on anatomical landmarks. Information extracted from other regions will also be important for the KA MTLE model, because of the interconnection between brain areas. Due to its size, the entire mouse hemisphere can be

scanned in one step, whereas the rat brain for example requires a more time consuming multi-step scanning approach. In terms of biological properties, the KA injection induces well-described morphological changes. Their investigation will be a benchmark to the visualization model, but also allow a more precise assessment of neuronal death and an accurate estimation of granular cell dispersion. These histological findings are evaluated in a limited number of 2D slices, making the method vulnerable to sampling error and reducing its statistical robustness.

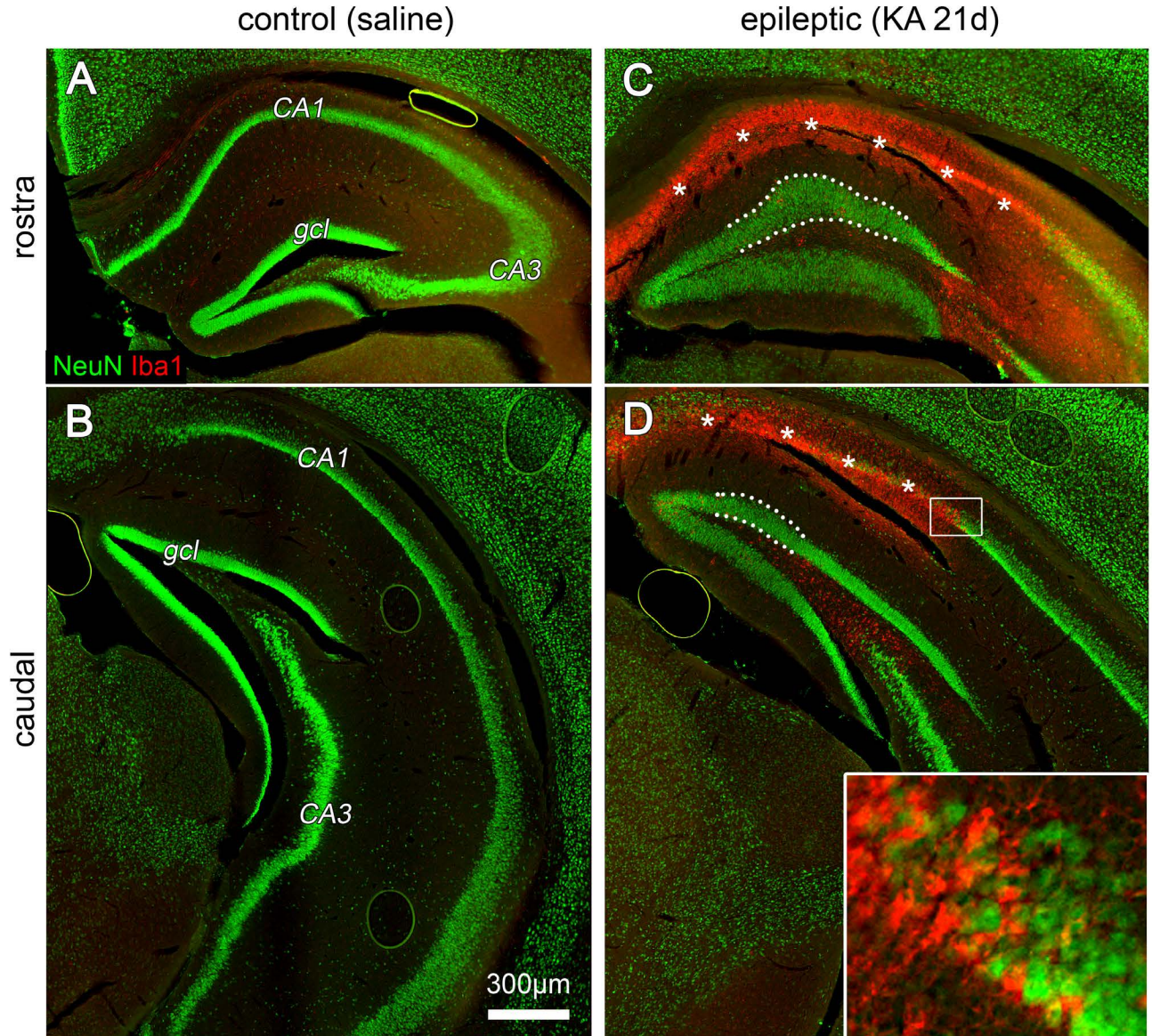


Figure 1: Morphological abnormalities observed in the epileptic mouse hippocampus. Neuronal loss (diminished green fluorescent signal (NeuN)) mainly in the CA1 region of epileptic mice is followed by microglia proliferation in the same region (red fluorescent signal (Iba1)). Granular cell dispersion is also visible both by the increase of the DG (gcl) thickness as well as the decrease in its fluorescent signal density.

2. MATERIALS AND METHODS

2.1 Kainate-induced MTLE

The chosen mouse model is the KA-induced MTLE model. It relies on the stereotaxic injection of kainate into the hippocampus, inducing an initial status epilepticus and subsequent clinical and morphological changes closely resembling those in human [19-21]. The onset and progress of epilepsy is monitored by electroencephalography (EEG) after electrode implantation. Following paraformaldehyde fixation, the extracted mouse brain hemispheres were provided for synchrotron radiation-based tomography measurements. Brains from healthy and KA-injected mice have been obtained, with three replicates per group, as schematically illustrated in Figure 2. The total number of provided brains was 14, in four groups of three replicates and one group of two replicates (one mouse died before its programmed sacrifice timepoint).

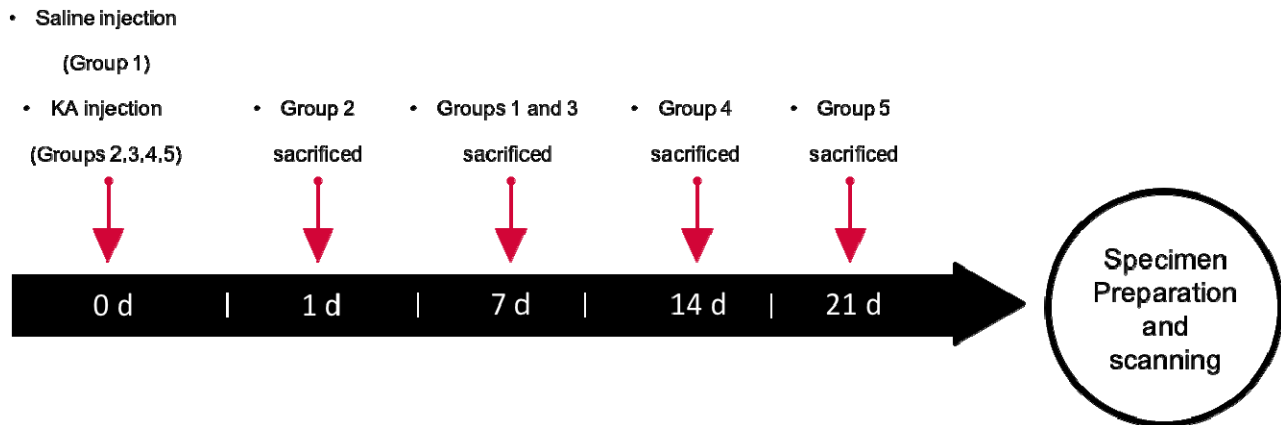


Figure 2. Scheme of timeline: Important time points for the cross-sectional MTLE experiment. One mouse from group 3 died before sacrifice.

2.2 Specimen preparation

Following preparation, isolated mouse brains were fixed in 4 % histological-grade buffered paraformaldehyde. Using a surgical scalpel, the hemispheres were separated along the middle line and in addition, the olfactory bulb and cerebellum were removed. Following a standard pathology protocol, the 28 brain hemisphere samples were dehydrated in ethanol, transferred to xylene and embedded in a paraffin/plastic polymer mixture (Surgipath Paraplast®, Leica Biosystems), giving a total of 4 standard paraffin blocks, containing one brain hemisphere each. Every block was then scanned using the laboratory X-ray imaging system nanotom@m (GE Sensing & Inspection Technologies GmbH, Germany) to validate sample preparation quality and assess the amount of trapped air inside the paraffin block, as well as the presence of cracks, or possible highly absorbing debris embedded together with the hemisphere inside the block. Melting of the paraffin blocks and re-embedding in paraffin was then performed as needed, until the embedding quality was deemed satisfactory for all paraffin blocks. Out of them, the cylindrical samples for the tomography measurement were extracted using a metal punch with an inner diameter of 6 mm and the cylindrical pieces were mounted on the special holders. For an overview of the specimen preparation procedure, see sequence of images in Figure 3.

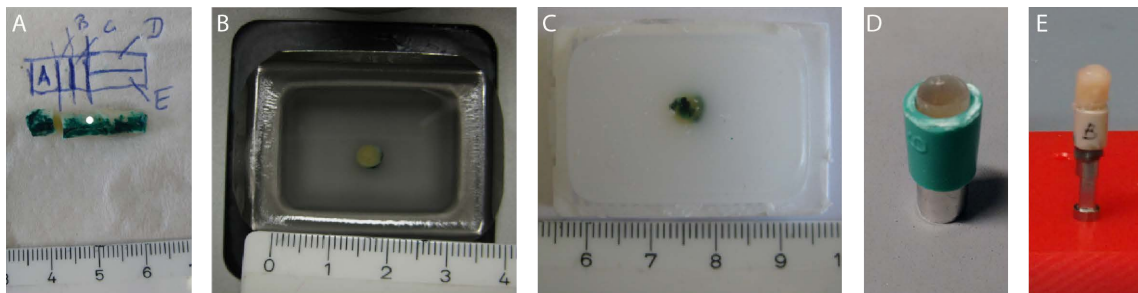


Figure 3. Specimen preparation: Paraformaldehyde-fixed tissue (A), tissue in liquid paraffin (B), tissue embedded in paraffin block (C), cylindrical specimen extracted using a biopsy punch (D) and mounted specimen ready for data acquisition (E).

2.3 Synchrotron radiation-based tomography measurements

Measurements were performed at the ID19 beamline (ESRF, Grenoble, France). A double grating setup was used for the X-ray grating interferometry (XGI) measurements. The beam-splitter grating had a mean periodicity of $4.785\ \mu\text{m}$ and a height of $29\ \mu\text{m}$, while the analyzer grating had a mean periodicity of $2.400\ \mu\text{m}$ and a height of $50\ \mu\text{m}$. The distance between gratings was $479.4\ \text{mm}$ and thus corresponded to the ninth fractional Talbot order. Used photon energy was $23\ \text{keV}$. For obtaining the radiographs, a lens-coupled scintillator and charge-coupled device (CCD) system was used, with an integrated 2048×2048 FReLoN 2K (Fast-Readout, Low-Noise, ESRF Grenoble, France) CCD. The effective pixel size corresponded to $5.1\ \text{mm}$. Over a range of 360 degrees, 1501 projections were obtained with four phase-stepping images recorded over one period of the interferometer fringe pattern for each projection angle, with an exposure time of $1\ \text{s}$. For single distance phase retrieval (SDPR) measurements, the effective pixel size was set to $1.74\ \mu\text{m}$ and the mean photon energy used was $19.45\ \text{keV}$. For acquiring the images, a 4421×4421 detector was used. Over a range of 360 degrees, $4,000$ projections were acquired for each scan.

3. RESULTS

3.1 Relation between XGI tomography and histological reference

The XGI tomography data with a pixel size of about $5\ \mu\text{m}$ were compared with the histological sections from the reference atlas of the mouse brain published by Paxinos and Franklin [22]. The hippocampus, thalamus, hypothalamus, cortex, and caudate putamen were easily recognized owing to the superior density resolution of the reconstructed phase contrast data. The ventricular spaces and vessels were also easily discernible, as exemplarily displayed in Figures 4 and 5 comparing the coronal and sagittal slices through the brain hemisphere with the corresponding Acetylcholinesterase histochemistry (AChE-) and Nissl-stained histological slices. A wide variety of anatomical microstructures are visible in the three-dimensional XGI data and because of the high contrast they are straightforwardly identified.

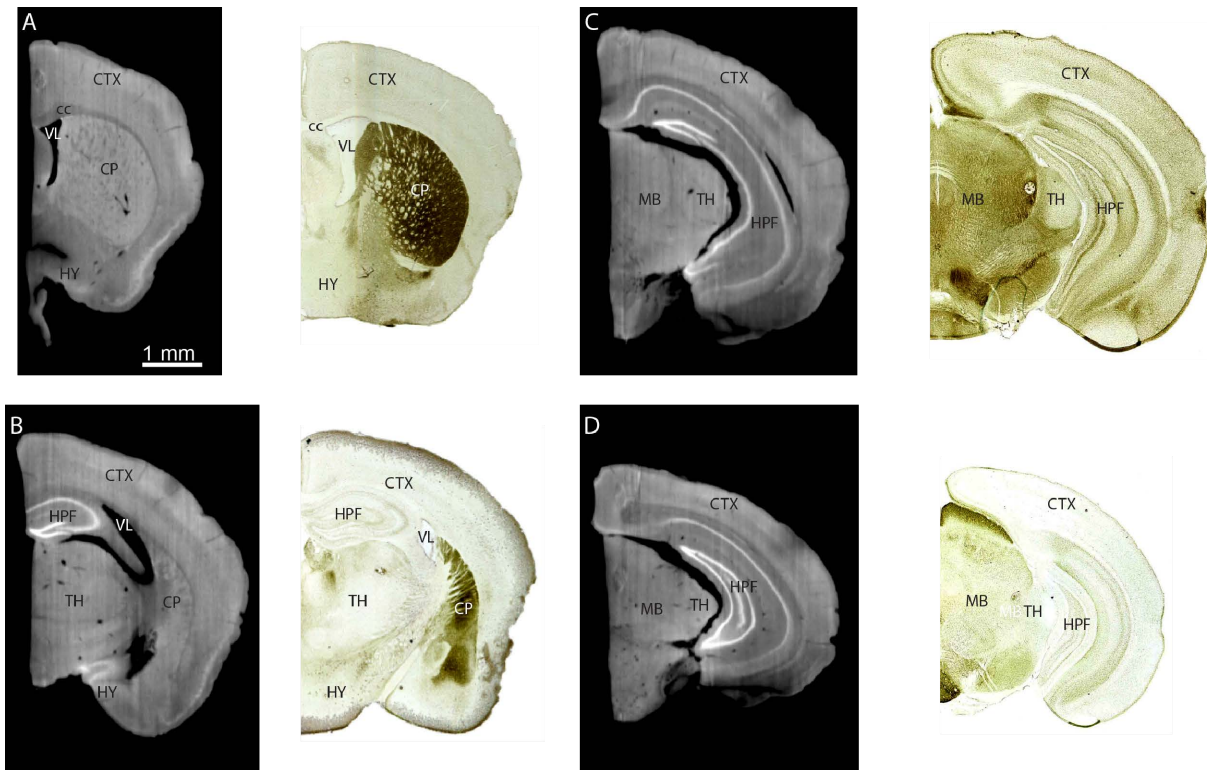


Figure 4. Comparison of X-ray grating interferometry (XGI) data with effective pixel size of $5.1\ \mu\text{m}$ to Acetylcholinesterase histochemistry (AChE) stained, coronal sections from literature [22]. CTX: Cerebral cortex, CP: Caudate putamen, cc: corpus callosum, HPF: Hippocampal formation, HY: Hypothalamus, MB: Midbrain, TH: Thalamus, VL: lateral ventricle

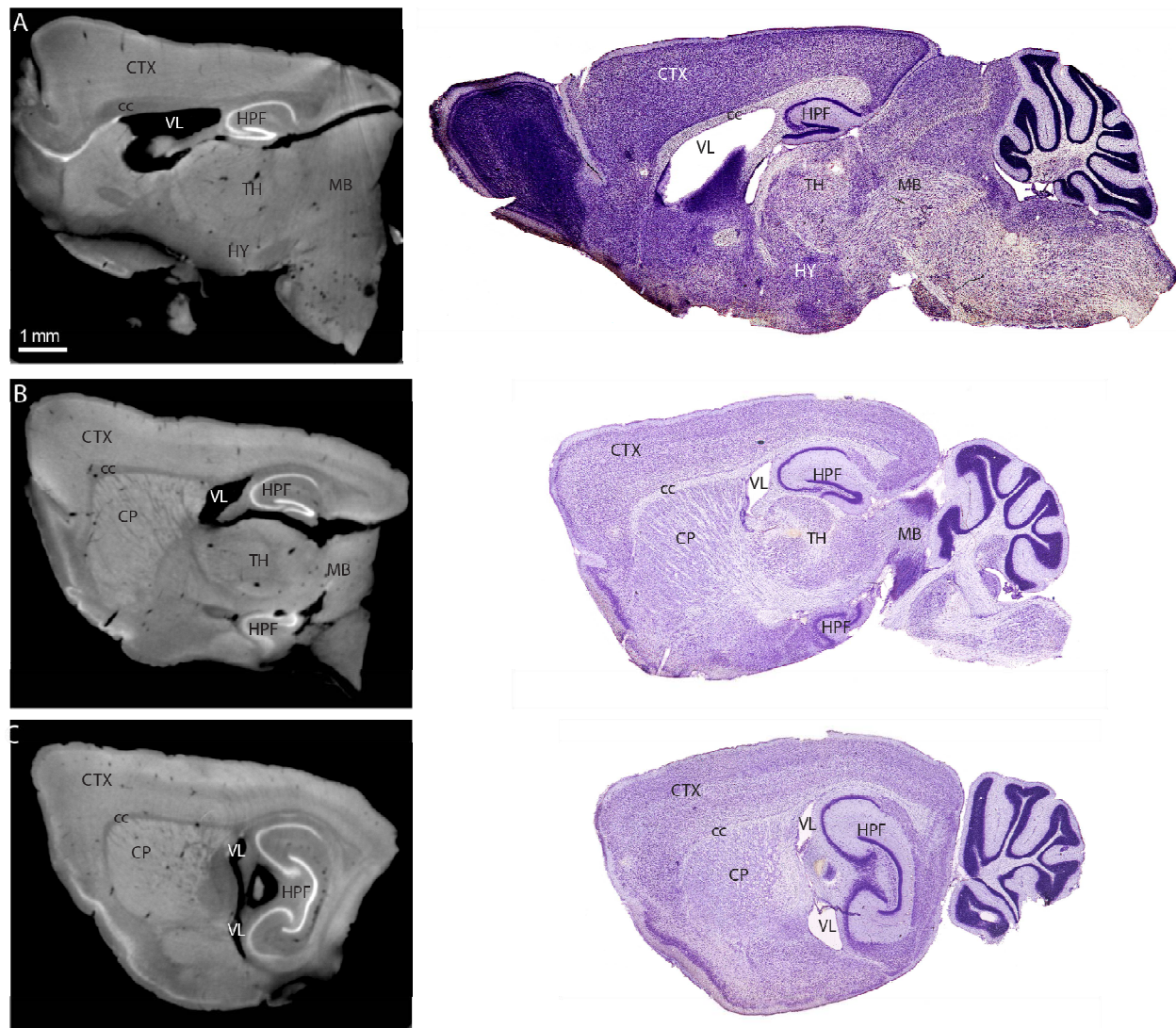


Figure 5. Comparison of X-ray grating interferometry (XGI) data with an effective pixel size of $5.1 \mu\text{m}$ to Nissl-stained sagittal sections from Paxinos and Franklin [22]. CTX: Cerebral cortex, CP: Caudate putamen, cc: corpus calosum, HPF: Hippocampal formation, HY: Hypothalamus, MB: Midbrain, TH: Thalamus, VL: lateral ventricle.

3.2 Semi-automatic segmentation of anatomical structures and volumetry of XGI imaging data

The reconstructed XGI data were visualized using the visualization software VGStudioMax 2.1 (Volume Graphics GmbH, Germany). By means of the relatively simple intensity-based segmentation tools the structures of interest were extracted. For the entire mouse hemisphere and the hippocampus, the histogram-thresholding was sufficient to obtain a reasonable estimate. Manual corrections, especially for streak artifacts, supported the refinement of the estimate.

For the ventricular spaces, vessels, and the caudate putamen, we applied a region-growing tool with manually selected seeding points. The results are represented in the images of Figure 6. Subsequent to the segmentation of these structures of interest, their volume was calculated. It is found that these quantities correspond to the literature values. The measured volumes were 163.5 mm^3 for the entire brain hemisphere, 16.4 mm^3 for the hippocampus, 20.0 mm^3 for the caudate putamen and 97.1 mm^3 for the ventricular spaces and vessels.

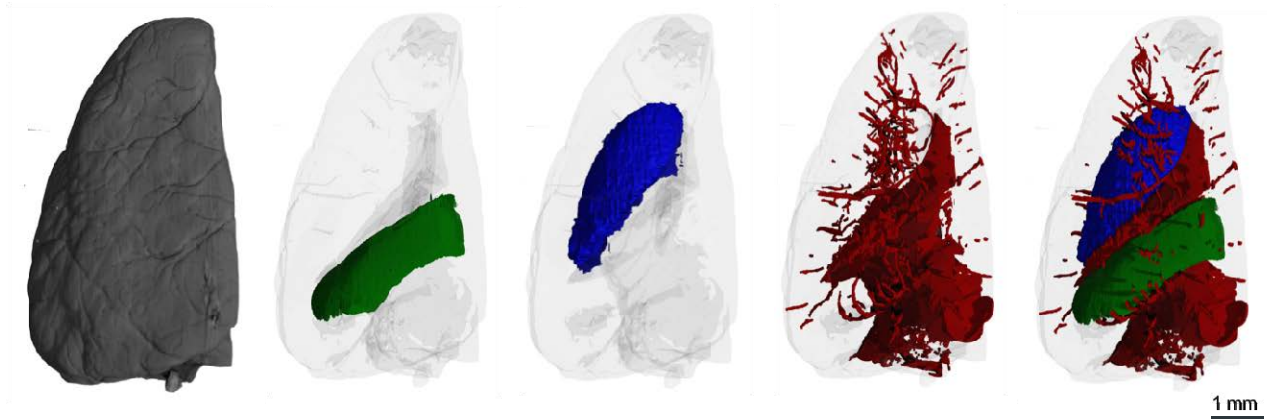


Figure 6. Segmentation of the anatomical structures of interest: entire mouse brain hemisphere (gray), hippocampus (green color), caudate putamen (blue color), ventricular spaces and vessels (red color).

3.3 Single-distance phase retrieval (SDPR)

The results of SDPR measurements allow for the identification of single cells in many parts of the mouse brains, which include the hippocampus. The cells were also visible after a reconstruction of the projections binned with a factor of three. Such a choice leads to an effective pixel size analogue to the generated XGI data (5.1 μm). Figure 7 compares selected virtual cuts and shows the influence of binning.

3.4 Initial comparison of XGI and SDPR

The aim of this pilot study was to compare the efficacy of XGI and SDPR for the purpose of the planned MTLE mouse experiment. Towards that end, we summarized the specific characteristics of each imaging modality that are of importance for our MTLE experiment. In detail, XGI shows increased density resolution that allows for the segmentation of basic anatomical structures. Nevertheless, identification of individual neurons is problematic and the scanning times are 3-4 hours per specimens. On the other hand, SDPR is around 4-5 faster, which is of increased importance for the case of high throughput experiments like the one we have planned. Artefacts due to trapped air are also attenuated in SDPR compared to XGI. On the other hand, the smaller pixel size is associated with bigger data and more demanding ring artefact removal process is also needed.

Table 3. Decision factors for choosing between XGI and SDPR

XGI with 5 μm pixels	SDPR with 1.75 μm pixels
Advantages	Advantages
Identification of basic anatomical structures Semi-automatic segmentation feasible	Scanning times of 45 min allow for high throughput. Lesser artifacts due to air trapped in paraffin
Disadvantages	Disadvantages
Scanning times of three to four hours Cell identification and segmentation demanding	Datasets bigger than 20 TB Demanding ring artifact removal

4. DISCUSSION

4.1 Expected results for the MTLE mouse model experiment

The combination of XGI and SDPR imaging of mouse brains will enable us to determine the pyramidal neuron loss in the CA1 to CA3 regions, the loss of large hilar cells, the loss of interneurons within the whole sclerotic part of the septal to intermediate hippocampus and the onset of GCD. The numerical quantification of these findings will demonstrate the advantage of the automated three-dimensional approach related to the histological stereological assessment.

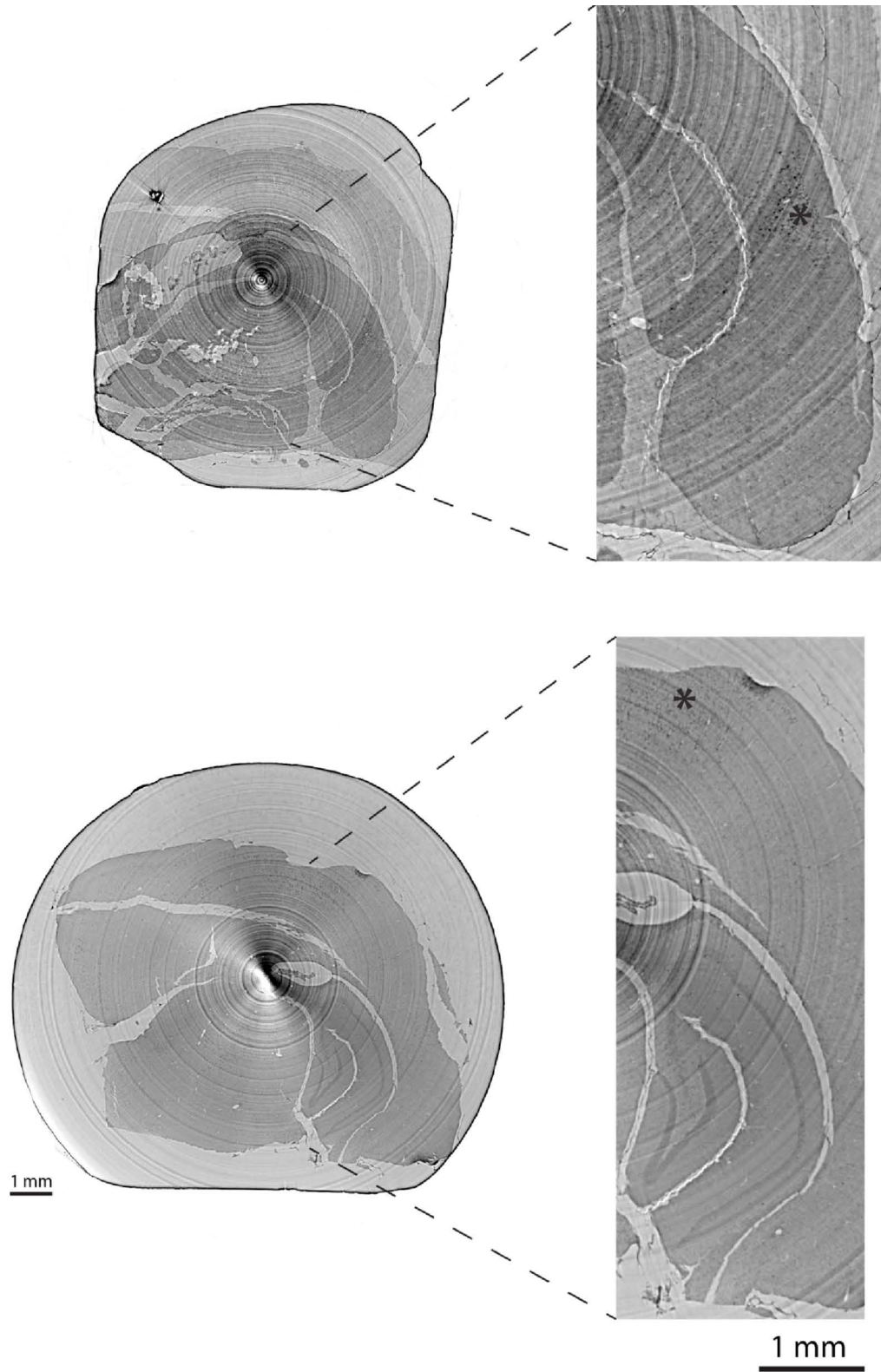


Figure 7. Single-distance phase retrieval (SDRP) results, showing a spatial and density resolution to make visible clusters of single cells (*): non-binned data (top) and threefold binned data (bottom).

Expected results also include the visualization of glial scarring in the epileptic hippocampus, the reduced total volume due to cell loss and the generation of a dense axonal plexus of sprouting mossy fibers. Based on the technique-specific advantages of phase-contrast tomography we also expect the accurate determination of the KA injection site and its morphology, an important issue concerning the spatial extent of structural changes, allowing better assessment of the KA treatment. We further aspire to an accurate, direct electrode position determination, which is more precise than the indirect histological assessment currently performed. It will allow for the better interpretation of EEG findings that strongly depend on local tissue reorganization [16]. In addition to that, the qualitative comparison between mouse and human hippocampal tissues could provide further insight into the analogy of morphology changes in MTLT between the two species. On a more general note for all animal model experiments, we also offer the possibility of additional information through data integration by correlating tomography to histology results [23]. Extracting more details from a given number of mice can reduce the size of mice group needed for statistically significant results. This reduction in animal group size is always a welcome development both for practical but also for ethical reasons.

4.2 Clinical relevance

We aim to extend the three-dimensional information on brain anatomy down to individual cells, while still allowing for established histology protocols. As hard X-ray phase tomography and histological evaluation are complementary modalities, one can reasonably assume additional findings and volumetric quantification. To underline the importance of acquiring and evaluating such tomography information for any model mouse in a robust way, we consider the case of MTLT: acquiring details on the changes of hippocampal lamination and neuronal population in each layer will significantly assist the study of pathogenesis and disease progression. More importantly, there is great promise in adjusting the existing and developing future therapeutic interventions. For example, the positive effect of coronal DG and hilus transection has already been observed in mice [24], while minimally invasive techniques such as gamma knife or focused ultrasound are validated alternatives to hippocampectomy [25]. A detailed visualization of the entire mouse hemisphere down to cellular level will thus greatly benefit models of such minimally invasive therapeutic interventions, with direct clinical implementation. Other neurobiology models that could benefit are the transgenic tau animal models and any neurodegenerative disease model, where cell loss is observed and can be better quantified in the whole brain. The detailed three-dimensional visualization of the entire brain would also address the general heterogeneity challenge between members of the same group in animal studies, a source of considerable sampling error when histology is performed, significantly affecting the final results obtained.

5. CONCLUSION

5.1 Expected results for the MTLT mouse model experiment

The combination of the XGI and SDPR imaging modalities is proposed for the case of cross-sectional mouse model studies, with the KA MTLT model on mice intended to be used as a benchmark. The complementarity between these two modalities is going to be exploited, combining the increased density resolution and quantitative nature of XGI with the true cellular resolution, reduced scanning times and flexibility offered by reconstruction with dedicated parameters that is offered by SDPR. At a later stage, the complementarity of these X-ray micro-tomography techniques with the gold standard of histology will be proven important towards a better integration into biomedical applications. It should be kept in mind that for animal model experiments the number of tissue samples to be scanned increases considerably, especially when compared to experiments focusing mainly on the technical novelties and advancements in X-ray imaging. As a consequence, special care should be taken in establishing a suitable methodology for conducting such experiments, including the adaptation and standardization of existing histological treatment protocols, so that the specimen preparation for synchrotron radiation-based measurements remains backwards compatible with the standard histological approach.

ACKNOWLEDGMENTS

The authors acknowledge the financial help of the Swiss National Science Foundation (SNSF) via projects 147172, 150164 and the R'Equip project 133802, as well as the ESRF for providing beamtime (application MD 896).

REFERENCES

- [1] Tomer, R., Ye, L., Hsueh, B., and Deisseroth, K., "Advanced CLARITY for rapid and high-resolution imaging of intact tissues," *Nat Protoc* 9(7), 1682-97(2014)
- [2] Chung, K., Wallace, J., Kim, S.-Y., Kalyanasundaram, S., Andalman, A. S., Davidson, T. J., Mirzabekov, J. J., Zalocusky, K. A., Mattis, J., Denisin, A. K., Pak, S., Bernstein, H., Ramakrishnan, C., Grosenick, L., Gradinaru, V., and Deisseroth, K., "Structural and molecular interrogation of intact biological systems," *Nature* 497(7449), 332-337(2013)
- [3] Schulz, G., Weitkamp, T., Zanette, I., Pfeiffer, F., Beckmann, F., David, C., Rutishauser, S., Reznikova, E., and Muller, B., "High-resolution tomographic imaging of a human cerebellum: comparison of absorption and grating-based phase contrast," *Journal of the Royal Society Interface* 7(53), 1665-1676(2010)
- [4] Zanette, I., Weitkamp, T., Lang, S., Langer, M., Mohr, J., David, C., and Baruchel, J., "Quantitative phase and absorption tomography with an X-ray grating interferometer and synchrotron radiation," *Physica Status Solidi A* 208 (11), 2526-2532(2011)
- [5] Hieber, S. E., Bikis, C., Khimchenko, A., Schweighauser, G., Hench, J., Chicherova, N., Schulz, G., and Muller, B., "Tomographic brain imaging with nucleolar detail and automatic cell counting," *Sci Rep* 6, 32156(2016)
- [6] Bohacek, J., Farinelli, M., Mirante, O., Steiner, G., Gapp, K., Coiret, G., Ebeling, M., Duran-Pacheco, G., Iniguez, A. L., Manuella, F., Moreau, J. L., and Mansuy, I. M., "Pathological brain plasticity and cognition in the offspring of males subjected to postnatal traumatic stress," *Mol Psychiatry*, (2014)
- [7] Huang, C. H., Pei, J. C., Luo, D. Z., Chen, C., Chen, Y. W., and Lai, W. S., "Investigation of gene effects and epistatic interactions between Akt1 and neuregulin 1 in the regulation of behavioral phenotypes and social functions in genetic mouse models of schizophrenia," *Front Behav Neurosci* 8, Published online(2014)
- [8] Sauer, J. F., Struber, M., and Bartos, M., "Impaired fast-spiking interneuron function in a genetic mouse model of depression," *Elife* 4, In press(2015)
- [9] Witsch, J., Golkowski, D., Hahn, T. T., Petrou, S., and Spors, H., "Cortical Alterations in a Model for Absence Epilepsy and Febrile Seizures: In Vivo Findings in Mice Carrying a Human GABA(A)R Gamma2 Subunit Mutation," *Neurobiol Dis*, In press(2015)
- [10] Engel, J., Jr., "Mesial temporal lobe epilepsy: what have we learned?," *Neuroscientist* 7(4), 340-52(2001)
- [11] Houser, C. R., "Granule cell dispersion in the dentate gyrus of humans with temporal lobe epilepsy," *Brain Res* 535(2), 195-204(1990)
- [12] Armstrong, D. D., "The neuropathology of temporal lobe epilepsy," *J Neuropathol Exp Neurol* 52(5), 433-43(1993)
- [13] Mello, L. E., Cavalheiro, E. A., Tan, A. M., Kupfer, W. R., Pretorius, J. K., Babb, T. L., and Finch, D. M., "Circuit mechanisms of seizures in the pilocarpine model of chronic epilepsy: cell loss and mossy fiber sprouting," *Epilepsia* 34(6), 985-95(1993)
- [14] Kowalski, J., Geuting, M., Paul, S., Dieni, S., Laurens, J., Zhao, S., Drakew, A., Haas, C. A., Frotscher, M., and Vida, I., "Proper layering is important for precisely timed activation of hippocampal mossy cells," *Cereb Cortex* 20(9), 2043-54(2010)
- [15] Marx, M., Haas, C. A., and Haussler, U., "Differential vulnerability of interneurons in the epileptic hippocampus," *Front Cell Neurosci* 7, Published online (2013)
- [16] Haussler, U., Bielefeld, L., Fropiep, U. P., Wolfart, J., and Haas, C. A., "Septotemporal position in the hippocampal formation determines epileptic and neurogenic activity in temporal lobe epilepsy," *Cereb Cortex* 22(1), 26-36(2012)
- [17] Schulz, G., Waschkies, C., Pfeiffer, F., Zanette, I., Weitkamp, T., David, C., and Muller, B., "Multimodal imaging of human cerebellum - merging X-ray phase microtomography, magnetic resonance microscopy and histology," *Scientific Reports* 2, Published online(2012)
- [18] Lévesque, M., and Avoli, M., "The kainic acid model of temporal lobe epilepsy," *Neuroscience & Biobehavioral Reviews* 37(10, Part 2), 2887-2899(2013)
- [19] Bouilleret, V., Ridoux, V., Depaulis, A., Marescaux, C., Nehlig, A., and Le Gal La Salle, G., "Recurrent seizures and hippocampal sclerosis following intrahippocampal kainate injection in adult mice: electroencephalography, histopathology and synaptic reorganization similar to mesial temporal lobe epilepsy," *Neuroscience* 89(3), 717-29(1999)

- [20] Riban, V., Bouilleret, V., Pham-Le, B. T., Fritschy, J. M., Marescaux, C., and Depaulis, A., "Evolution of hippocampal epileptic activity during the development of hippocampal sclerosis in a mouse model of temporal lobe epilepsy," *Neuroscience* **112**(1), 101-11(2002)
- [21] Heinrich, C., Nitta, N., Flubacher, A., Muller, M., Fahrner, A., Kirsch, M., Freiman, T., Suzuki, F., Depaulis, A., Frotscher, M., and Haas, C. A., "Reelin deficiency and displacement of mature neurons, but not neurogenesis, underlie the formation of granule cell dispersion in the epileptic hippocampus," *J Neurosci* **26**(17), 4701-13(2006)
- [22] [The Mouse Brain in Stereotaxic Coordinates] Academic Press, (2008).
- [23] Stalder, A. K., Ilgenstein, B., Chicherova, N., Deyhle, H., Beckmann, F., Müller, B., and Hieber, S. E., "Combined use of micro computed tomography and histology to evaluate the regenerative capacity of bone grafting materials," *International Journal of Materials Research* **105**(7), 679-691(2014)
- [24] Pallud, J., Haussler, U., Langlois, M., Hamelin, S., Devaux, B., Deransart, C., and Depaulis, A., "Dentate gyrus and hilus transection blocks seizure propagation and granule cell dispersion in a mouse model for mesial temporal lobe epilepsy," *Hippocampus* **21**(3), 334-43(2011)
- [25] Quigg, M., and Harden, C., "Minimally invasive techniques for epilepsy surgery: stereotactic radiosurgery and other technologies," *J Neurosurg* **121 Suppl**, 232-40(2014)